THE ASTROPHYSICAL JOURNAL, 481:532–544, 1997 May 20

TIME EVOLUTION OF SOLAR MICROWAVE BURSTS

L. BELKORA[1]
University of Colorado, Department of Astrophysics, Planetary, and Atmospheric Science, Boulder, CO 80309-0391
Received 1996 July 8; accepted 1996 November 26

ABSTRACT

Spectra of solar microwave bursts often have a steeper slope than expected on the low-frequency side, manifest a low brightness temperature, and maintain a constant frequency of maximum brightness temperature ν_{peak}, despite the burst's evolution in peak brightness. We used a gyrosynchrotron code to model the emission from the flare of 1992 July 16, which exhibited these characteristics. We find that the Razin effect—the suppression of radiation from an electron in a medium in which the index of refraction is less than unity—accounts for the shape and evolution of the burst. Using data from the Owens Valley Solar Array we demonstrate that in a medium with density 2×10^{11} cm^{-3} and magnetic field 300 G, conditions not uncommon for solar microwave bursts, the gyrosynchrotron spectrum from mildly relativistic electrons can be suppressed for frequencies up to at least 10 GHz. We can then explain the constancy of ν_{peak}, the burst's low brightness temperature, and the steep low-frequency slope of the spectrum using a simple model in which only the density of accelerated electrons varies during the flare. Our model implies values for the density of accelerated and ambient electrons which are in agreement with those derived from X-ray data for this flare.

Subject headings: Sun: flares — Sun: particle emission — Sun: radio radiation

1. INTRODUCTION

The motivation to study the Razin effect in solar microwave bursts is the difficulty of explaining some well-known features of microwave continuum spectra. Models of solar microwave emission due to the gyrosynchrotron[2] mechanism (e.g., Dulk & Marsh 1982) fail to account for characteristics of some bursts: the steep low-frequency slope of the burst spectrum, the evolution of the spectrum in time, and the low brightness temperature before or after the peak. Ramaty & Lingenfelter (1967) noted some of these features in type IV meter to centimeter-wavelength emission, and Stähli, Gary, & Hurford (1989) calculated their rate of occurrence in a survey of microwave bursts. These earlier observations, however, were of flux or total power spectra, not the brightness temperature spectra of spatially resolved sources. Variation in source size could not be ruled out as a cause of the special features in the spectra.

The flare of 1992 July 16 provided a good data set to investigate the problem. The microwave burst was observed at the Owens Valley Solar Array (OVRO) (operated by the California Institute of Technology), a five-element radio telescope. From the flux and imaging data acquired during the rise and decay phases of the flare, we were able to determine the brightness temperature spectrum between 6 and 16 GHz. We selected spectra from six time samples, three during the rise phase and three during the decay phase, for further study (Belkora 1995; Belkora, Gary, & Kiplinger 1996). Complementary X-ray data for this event were available from the instruments on board the *Yohkoh* spacecraft.

A striking feature of these data is that the frequency of maximum brightness temperature ν_{peak} remains nearly constant (a shift of less than 2 GHz), while the peak brightness temperature varies over nearly 2 orders of magnitude. The model of Dulk & Marsh predicts an increase in ν_{peak} as the peak brightness temperature increases and shows a shallower slope on the low-frequency side than observed. Several authors have commented on the fact that observed spectra are often in disagreement with the model predictions on these points (see, e.g., Stähli et al. 1989 and Benka & Holman 1992). In the survey of microwave bursts conducted by Stähli et al. (1989), only two events, or 4% of the sample, showed a shift in ν_{peak} as large as that expected from theory.

An appealing explanation for the appearance of the spectra is that a low-frequency cutoff is at work. Figure 1 illustrates how a low-frequency cutoff can produce steep slopes on the low-frequency side of the turnover and an apparently constant ν_{peak}.

In our analysis we considered whether the Razin effect (e.g., Ginzburg & Syrovatskii 1965; Ramaty & Lingenfelter 1967) might provide the required low-frequency cutoff. The Razin effect is the suppression of radiation in a medium with index of refraction less than unity. Razin suppression is not a propagation effect; it is a suppression of emission at the source, and, as pointed out by Ramaty (1969), it leads to a corresponding reduction in the absorption process. This means that medium suppression and gyrosynchrotron reabsorption must be treated consistently in modeling the emission.

Klein (1987) has also considered the role of Razin suppression in solar microwave sources and finds, as we do, that it is an important effect. Our results differ on several points, for example, in the inferred density of ambient and accelerated electrons. Our analysis (Belkora 1995) is the first to demonstrate Razin suppression in brightness temperature spectra using the rise and decay phases of a burst. Our explanation for the evolution of the spectrum in time is a key element of our argument for the importance of the Razin effect.

We used a gyrosynchrotron code described by Ramaty, Schwartz, & Nakajima (1994) to model the flare emission,

[1] Presently at Fermilab, Mail Station 206, P.O. Box 500, Batavia, IL 60510.

[2] We use the terms "gyrosynchrotron" or "gyroresonance emission" for synchrotron radiation at low energy, $\gamma \sim 2$ or 3, i.e., between cyclotron and synchrotron energies.

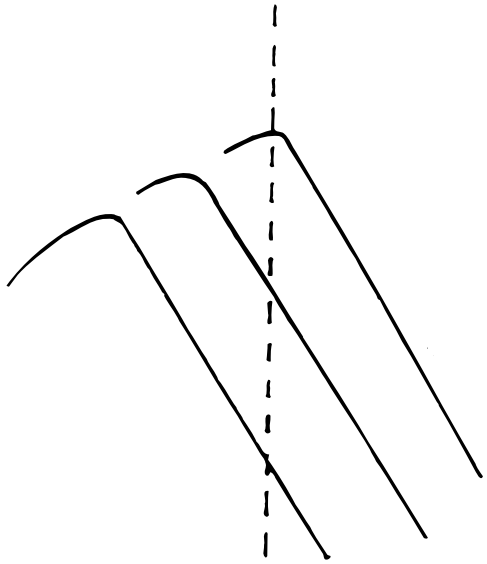

FIG. 1.—Sketch to illustrate how a low-frequency cutoff (*dashed line*) can produce an apparently constant peak frequency and steep low-frequency slope.

taking the Razin effect into account. We describe our observations in § 2, numerical modeling in § 3, and present our discussion and conclusions in §§ 4 and 5.

2. OBSERVATIONS

The flare occurred in Active Region 7220, 63 degrees west of disk center and 10 degrees south. The microwave burst peaked near 16:55 UT, following a rise phase of less than 1 minute. The initial decay occurred in about 1 minute also, but low-level flux enhancement persisted for several minutes. Instruments on the *Yohkoh* and *GOES* satellites observed the flare, as well as the Owens Valley Solar Array. The flare had a soft X-ray classification of M6.8.

2.1. *Brightness Temperature Spectra*

Data from the Owens Valley Solar Array (see, e.g., Hurford, Read, & Zirin 1984) are originally in the form of correlated phase and amplitude between seven antenna pairs, and total power is measured independently by two of the dishes. The observing mode we used yielded visibilities in both left circular polarization (LCP) and right circular polarization (RCP) at 45 frequencies between 1.0 and 18.0 GHz. In practice, data above 16.4 GHz rarely survived the automatic flagging of bad data (for bad tracking by the dishes, or lack of phase lock in the receivers, for example). The data are calibrated for daily and monthly phase variations by reference to the calibrator sources.

Before making images from the data we selected a time period just prior to the flare and vector-subtracted the spectrum corresponding to this time period from all subsequent data, which removed the emission spectrum of the underlying active region. The subtracted spectrum has very low amplitude compared to that at the peak of the flare, and the emission to which it corresponds is too complex to map in the snapshot data; to image the active region requires a long-time integration, usually 4 hr or more. However, the preflare subtraction is useful to isolate the flare spectrum from the active region spectrum during the times of relatively low level emission. We select the time interval for preflare subtraction by examining the time plots at many different frequencies and finding the latest time before the flare which shows no systematic change in the amplitude.

We selected three time intervals during the rise phase of the flare (A, 16:54:53–16:55:04 UT; B, 16:55:05–16:55:16 UT; C, 16:55:29–16:55:40 UT) and three during the decay phase (D, 16:56:41–16:56:52 UT; E, 16:57:05–16:57:16 UT; F, 17:00:05–17:00:52 UT) and carried out the "clean" procedure (see, e.g., Cornwell & Braun 1989) on single-frequency maps for these times. Unfortunately, the LCP data were largely unusable for further analysis because of a combination of technical problems and the fact that the source appears to have been more complex in LCP than in RCP. On several baselines and at intermittent times the correlated amplitude values were anomalously low. In some cases the data from one or more baselines are missing. This problem does not prevent us from forming images, but it leads to inadequately sampled flux and, hence, misleading brightness temperature values.

We attempted to "clean" maps below 6 GHz but found that the source is complex and substantially overresolved at the lower frequencies. The comparison of total power with the correlated amplitude measured on the shortest baseline is our guide to determining whether or not a source is overresolved.

Even above 6 GHz, we found that the source was not resolved at all times and at all frequencies. For this reason we applied a correction factor to the inferred brightness temperature of the affected data points. We determined the correction by deconvolving the source size from the observed source and the interferometer beam. We used the deconvolved source size to correct for the filling factor of the source in the beam. (See Belkora 1995 for a complete description of the method.) At the peak of the flare, when the correction was greatest, the correction amounts to an increase in the inferred brightness temperature by a factor of 1.6.

Figure 2 is a log-log plot of the brightness temperature spectra for each of the six time samples. The uncorrected brightness temperatures are denoted by crosses and the corrected ones by squares. The correction we made for the filling factor of the source in the beam raised the overall brightness temperature at the peak of each spectrum but did not substantially affect the shape of the spectra. This fact is important because we are more concerned with modeling the shape of the burst spectrum and its evolution in time, rather than fitting each spectrum precisely.

The brightness temperature at the spectral turnover ranges from about 2×10^7 K to 5.5×10^8 K and back down to about 1×10^7 K. At the same time, the frequency of peak emission, $\nu_{\rm peak}$, varies by less than 2 GHz. The low-frequency slope of the spectrum is not as well defined as $\nu_{\rm peak}$ because of the small number of points to the left of the peak. For spectrum C, the low-frequency slope using the corrected data is 4.0.

2.2. *Difficulty of Explaining the Spectra Using Simplified Theory*

Dulk & Marsh (1982) explored gyrosynchrotron emission from mildly relativistic electrons with energy in the range $\sim$10 keV to $\sim$1 MeV. Electrons with energy in this range play a role in radio and hard X-ray emission from solar flares. The authors sought approximations to the theoretical expressions for gyrosynchrotron emission from

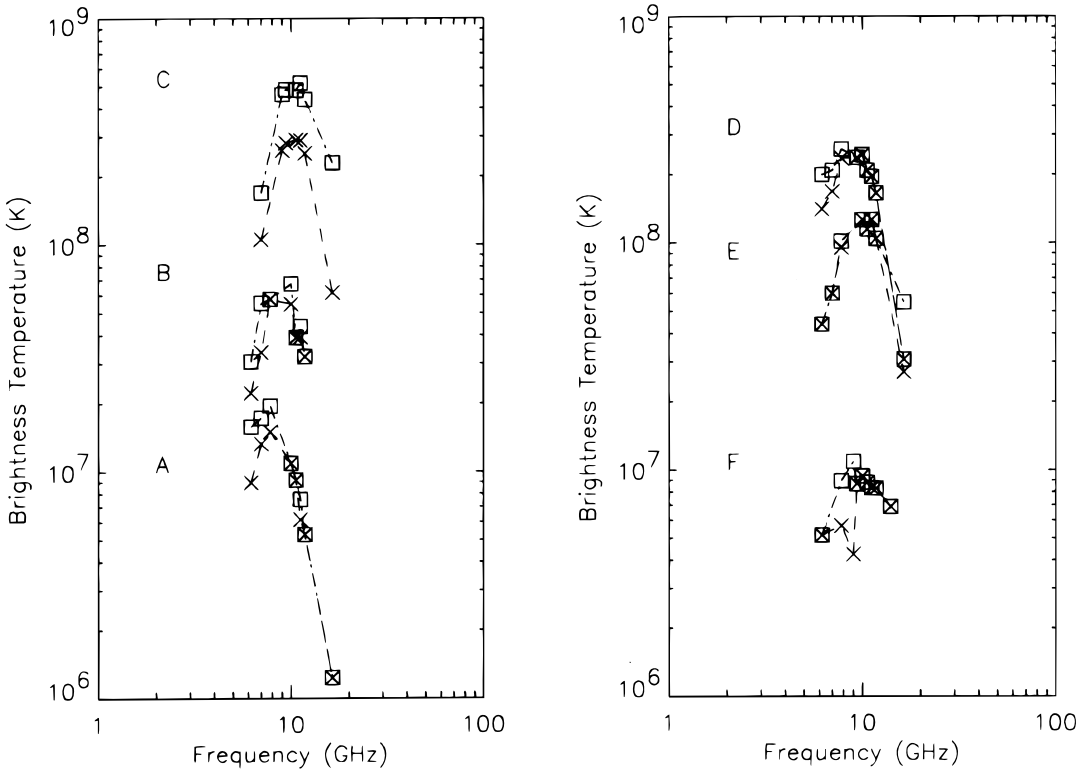

FIG. 2.—Microwave burst spectra from the flare of 1992 July 16, together with model fits to the data. *Left*, rise phase of flare; *right*, decay phase of flare. The data were corrected for the filling factor of the source in the beam. The corrected points are shown by square symbols.

these particles. For their numerical calculations the authors used formulae developed for the widely applicable case in which the index of refraction n is near unity. As noted by the authors, ignoring deviations of n from unity implies that Razin suppression is unimportant in the cases they examine.

We use the results of Dulk & Marsh to estimate the shift in $\nu_{\rm peak}$ we would expect for the increase in brightness temperature that occurs in our flare. Extrapolating the $T_{\rm eff}$ curve in their Figure 3*c*, we find that a peak T_b of 2×10^7 K would occur at a frequency $\nu/\nu_B \sim 2$ (where ν_B is the gyrofrequency), while a peak T_b of 6×10^8 K would occur near $\nu/\nu_B \sim 8$. For higher peak brightness temperatures where their simplifying expressions are valid, a similar increase in T_b of a factor of 30 would lead to an even larger shift in the peak frequency, as can be seen from the low slope of the $T_{\rm eff}$ curve. The problem with the simplified theory of gyrosynchrotron emission is immediately apparent because the observed shift in peak frequency for the burst studied here is less than 2 GHz.

Some low-frequency absorption or cutoff is apparently needed to explain the observed spectra. As illustrated in the introduction, a low-frequency cutoff can produce a constant peak frequency and steep low-frequency slope. In the next section we investigate the possibility that the cutoff is provided by Razin suppression. Free-free absorption of gyrosynchrotron emission plays a role, as well; the high ambient density required for Razin suppression means that some free-free absorption must accompany it. However, our concern here is to determine to what degree the observed spectra may be explained by Razin suppression. X-ray data show that, indeed, the temperature of the flare plasma is too high to allow free-free absorption to account for the low-frequency cutoff in this particular flare.

3. NUMERICAL MODELING

3.1. *The Gyrosynchrotron Code*

We used a gyrosynchrotron code described in Ramaty et al. (1994) and provided to us by the lead author. The code is based on the equations for the gyrosynchrotron emission and absorption coefficients presented by Ramaty (1969) (except for the omission of a spurious term; see Ramaty et al. 1994). The code treats the case of a distribution of electrons radiating in a cold, collisionless, magnetoactive plasma. The index of refraction in the plasma depends on the gyrofrequency ν_B as well as the plasma frequency ν_p and frequency of observation ν; i.e., it is not assumed that the gyrofrequency is low and that the simpler form of the index of refraction ($n^2 = 1 - \nu_p^2/\nu^2$) pertaining to an isotropic plasma may be applied. The exact index of refraction used in the code has two forms corresponding to wave propagation in the ordinary (+) and extraordinary (−) modes, and is written as follows, where θ is the angle between the magnetic field and the direction of wave propagation:

$$\eta_{\pm}^2(\theta) = 1 + 2\nu_p^2(\nu_p^2 - \nu^2) \times \{\pm[\nu^4\nu_B^4 \sin^4\theta + 4\nu^2\nu_B^2(\nu_p^2 - \nu^2)^2 \cos^2\theta]^{1/2} - 2\nu^2(\nu_p^2 - \nu^2) - \nu^2\nu_B^2 \sin^2\theta\}^{-1} .$$

The importance of the use of the exact index of refraction is that when n differs from unity the medium affects the generation of radiation as well as its propagation and absorption, and this is taken into account by the code. The index of refraction may differ significantly from unity in one or both modes of propagation. We call the suppression of gyrosynchrotron radiation in a plasma when the index of refraction is less than unity the Razin effect.

We used Ramaty et al.'s code to evaluate the emission and absorption coefficients, and hence the brightness temperature, resulting from a power-law distribution of electrons with an isotropic pitch angle distribution. We now briefly describe the equations used and the input and output of the code. The volume emissivity corresponding to a single electron is obtained by summing the radiation over some range of harmonics s of the gyrofrequency, where the range of harmonics that is relevant is determined by the Lorentz factor γ and pitch angle ϕ of the electron as well as the index of refraction in the ambient medium. The volume emissivity of a single electron is integrated over the particle distribution function to obtain the total emissivity η. The reabsorption of photons by electrons in the magnetic field is written in terms of the emissivity by way of the Einstein coefficients, to give the absorption coefficient κ.

The inputs to the code are as follows. To define the ambient medium one specifies a uniform magnetic field strength, the cosine of the angle θ between the field and the line of sight, and the so-called Razin parameter $\alpha = 1.5\nu_B/\nu_p$ (Ramaty & Lingenfelter 1967). The α parameter serves as an index for the influence of the medium: Ramaty (1968) demonstrated with numerical models that the emission is suppressed when $\alpha\gamma < 1$. The density of the electrons in the ambient medium, which determines the plasma frequency, is set by α, since the field strength and hence the gyrofrequency is already specified.

To define the electron energy spectrum we specify the exponent δ and normalization factor A of the distribution function $N(E) = AE^{-\delta}$ (MeV^{-1}), as well as the lower and upper bounds of electron energy E_0 and $E_{\max}$ used in the integration over the distribution function, which in the analytic expression is carried out from $\gamma = 1$ to ∞. We also specify the angular size of the source, which is relevant when the total flux is of interest. Finally, we determine the range of observation frequencies examined by the code and the electron energy value at which the computation shifts from the full gyrosynchrotron formulation to the faster ultrarelativistic formulae of Ginzburg & Syrovatskii (1965) (see Ramaty et al. 1994).

The outputs include the x- and o-mode emissivities and absorption coefficients, the x- and o-mode flux densities at Earth, and the degrees of polarization. For our purposes we combined the emissivities and absorption coefficients and assumed a fixed path length to the source L to calculate the brightness temperatures in each of the two modes according to the formula

$$T_b = \frac{\eta_\nu}{\kappa_\nu}\frac{c^2}{\nu^2 k_B}(1 - e^{-\kappa_\nu L}) .$$

3.2. *Modeling the Results*

In this section we discuss the influence on the brightness temperature spectra of each of the input parameters, present the results for the fitting to the spectra, and note the effect of Razin suppression. We also remark on the validity of the simplified expressions of Dulk & Marsh for the peak brightness temperature and frequency of maximum emission for our particular flare. All of the results we discuss apply to the x-mode. Results for the o-mode are generally similar, but with lower intensity. Unfortunately, as noted in § 2.1, we were not able to make polarization measurements because of source complexity and other problems in the left circular sense of polarization (LCP). However, we were able to identify the mode corresponding to RCP from Marshall Space Flight Center magnetograms.

We begin by addressing the question of the uniqueness of the results of our fits to the data. We did not formally apply inverse theory to uncover the best fit to the data, but made a "first-order" determination of the gyrosynchrotron model parameters in a space that clearly constituted a global minimum in the model fit to the data.

The gyrosynchrotron model equations depend nonlinearly on a set of eight parameters. For the determination of the brightness temperature spectra these are δ, the exponent in the energy distribution function, B, the magnetic field strength, θ, the angle between the field and the line of sight, E_0, the low-energy cutoff in the electron energy spectrum, $E_{\max}$, the high-energy cutoff, α, which defines the ambient density; n_e (accel), the accelerated particle density, and L, the path to the source. The data to be fitted consist of seven, eight, or nine points in the spectrum, depending on the time sample. The B and C spectra consist of only seven data points, the A and E spectra of eight, and the D and F spectra of nine. Formally, then, the problem of fitting the model to the B and C spectra is underdetermined, although a priori information can be added to the problem, such as requiring the magnetic field to lie in the range from 10 to 1000 G, to aid in finding a solution.

We did not attempt an eight-dimensional grid search for the best fit to the data because our goal is to understand the shapes and evolution of the spectra, not to determine precise values of the parameters. We conducted a sensitivity analysis to understand the effects of the variables in the gyrosynchrotron model and used the results of the sensitivity analysis to locate the global minimum to the fit.

The sensitivity analysis is an investigation of the hierarchy of model parameters in terms of their influence and of the interplay of parameters. A given spectrum may be fitted, for example, with a magnetic field that is high or low, depending on the energy distribution function and densities of energetic and ambient electrons. However, our sensitivity analysis showed that some combinations of parameters that would be required to fit a feature of the spectrum, such as the peak frequency, corresponded to very unusual or artificial conditions. Ruling out those solutions is equivalent to adding a priori covariance in a formal model fitting. One advantage of our heuristic approach is that we did not have to think up all the possible a priori information ahead of time.

The evolution of the spectrum in time is a particularly strong constraint, as we shall see. Many of the alternative fits that we rejected would require two or more parameters to offset each other in just the right way to keep the peak frequency approximately constant. Such changes can be considered unlikely on the grounds of inordinate complexity.

Although the fits we derived look very good, as will be shown later in this section, we caution that the main import of our modeling is to explain the shape and evolution of the spectra and to derive an accurate first-order set of parameters, and not to determine precise values of the model inputs. In keeping with this philosophy, some limitations were imposed on the range of input parameters to speed the model fitting. For example, we kept the path length to the source constant at 10^9 cm and have stayed with a fixed lower bound to the integration in energy. We took the angle between the magnetic field and the line of sight to be 60°

because the active region was located about 60° from disk center, and it is fair to assume that the dominant component of the magnetic field was radial. These choices affect the details of the emitted spectrum. We have given some indication of the errors in our fits in quoting the results.

3.3. *Cartoon Results*

To help illustrate the influence of the various parameters on the shape of the spectrum we give a number of pictorial demonstrations. In Figures 3–9 we show the results of varying the eight free parameters in the gyrosynchrotron model. In each case the left panel illustrates the behavior of the free parameter in the presence of strong Razin suppression ($\alpha = 0.320$), and the panel on the right shows the behavior when $\alpha = 1$, when there is negligible suppression.

Figure 3 shows the effect of varying the accelerated particle density, with and without the effect of Razin suppression. All other parameters, such as magnetic field strength or the exponent in the energy distribution function, were kept constant. The accelerated particle density is one of the four dominant variables affecting the gyrosynchrotron spectrum, along with the Razin parameter α, the exponent δ in the energy distribution function, and the magnetic field B. The figure shows, in the case without Razin suppression, that the peak brightness temperature ranges from about 10^8 to about 2×10^9 K when the accelerated particle density is increased from 1 cm^{-3} to 10^7 cm^{-3}. If Razin suppression occurs with $\alpha = 0.320$, corresponding, in this case, to an ambient density of 2.6×10^{11} cm^{-3}, the change in peak brightness temperature is from 5×10^5 K to 2×10^9 K. The comparison of the two panels shows clearly the effect of Razin suppression: the low-frequency emission is suppressed, so that resonance structures are not apparent, and, because of the cutoff on the low-frequency side of the spectrum, the frequency of maximum emission remains constant.

Figure 4 shows the effect of varying δ, the index in the energy distribution function. In the absence of Razin suppression the peak of the curve moves toward higher frequencies and lower peak brightness temperature as the index is increased from 3 to 7. With Razin suppression the curves corresponding to lower indices are more affected, so that as δ increases, the curve initially moves up. Again, resonant structures are suppressed along with the low-frequency emission.

In Figure 5 B is varied from 50 to 450 G. Increasing B shifts the peak of the curve to the right because the harmonics of the gyrofrequency with high optical depth are shifted to higher frequencies, but the peak in the spectrum also shifts down to lower brightness temperature because the efficiency of the emitting process is reduced. In the curves with Razin suppression, the peak frequencies are slightly lower than in the curves without because the low-frequency side is cut off.

Figure 6 shows the effect of varying the high-energy cutoff in the energetic particle distribution from 0.32 MeV to 3.2 MeV. As the maximum energy level is increased, the peak brightness temperature increases slightly, and the bandwidth of the curve is broadened from the optically thin side.

Figure 7 shows the minimal effect of varying the low-energy cutoff, which in fact was not varied in our modeling. Electrons with energy below the cutoff contribute to the thermal background population. In Figure 7 we show that the minimum energy may range from 0.01 MeV to 0.1 MeV with no appreciable effect on the gyrosynchrotron spectrum

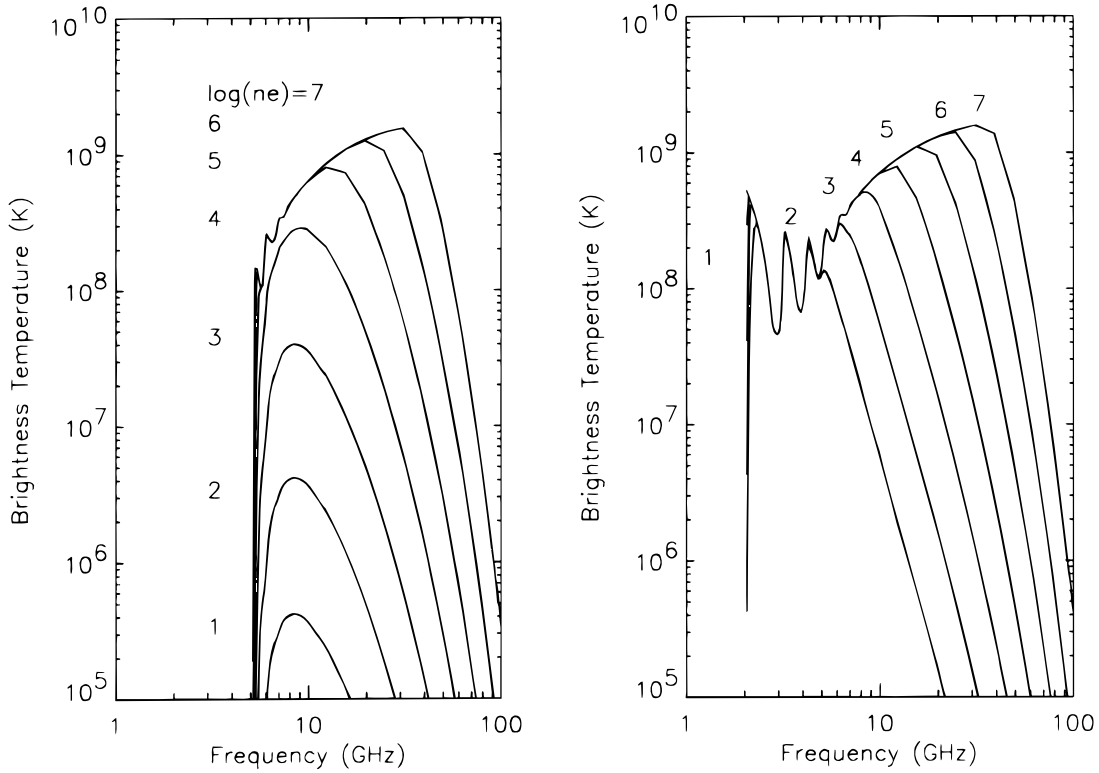

FIG. 3.—Effect on the brightness temperature spectrum of varying the density of accelerated particles from 10 to 10^7 cm^{-1}. The left panel ($\alpha = 0.320$) shows the effect with Razin suppression, and the right panel ($\alpha = 1.0$) shows the effect without Razin suppression.

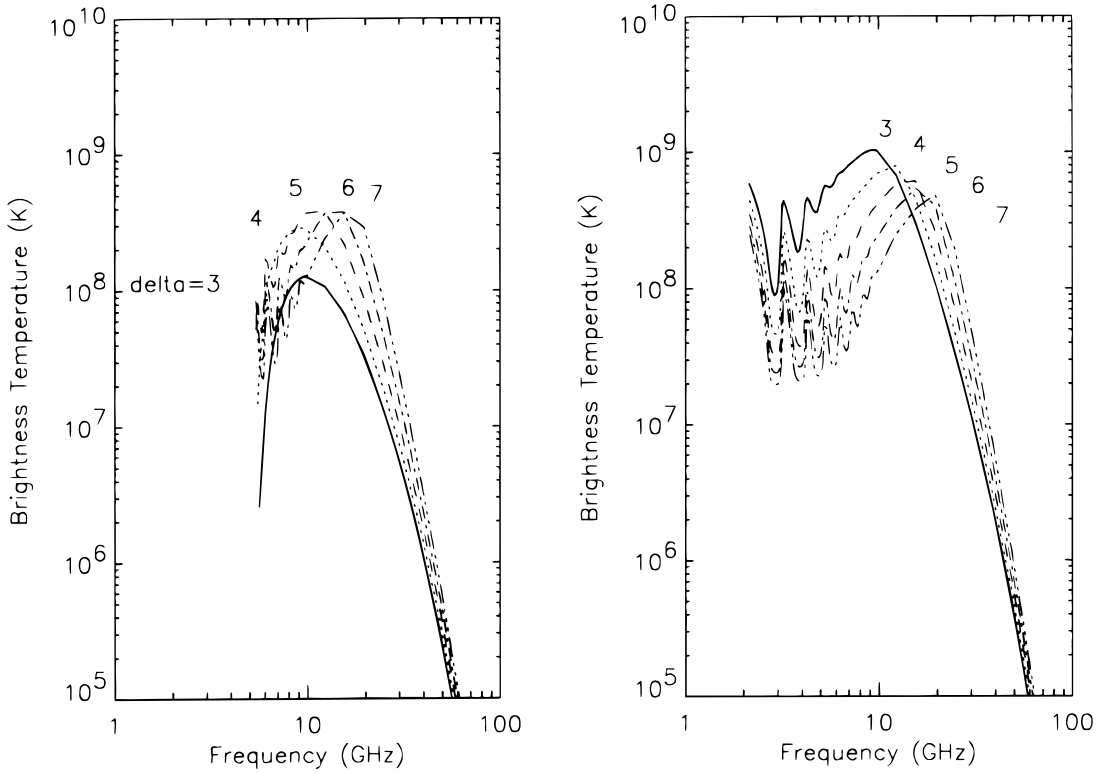

FIG. 4.—Effect on the brightness temperature spectrum of varying the exponent δ in the energy distribution function. The range of δ shown, from 3 to 7, is typical for microwave bursts. The left panel shows the effect with Razin suppression, and the right panel without.

in the case of strong Razin suppression. In the case of $\alpha = 1$, eliminating the lower energy electrons caused the resonant structures at low frequency to disappear. This result suggests that the gyrosynchrotron emission between 6 and 16 GHz is not strongly dependent on the electrons with energy in the range 0.01 MeV to 0.1 MeV.

Figure 8 shows the effect of varying the path length to the source. This is a large effect, but in practice it is related to

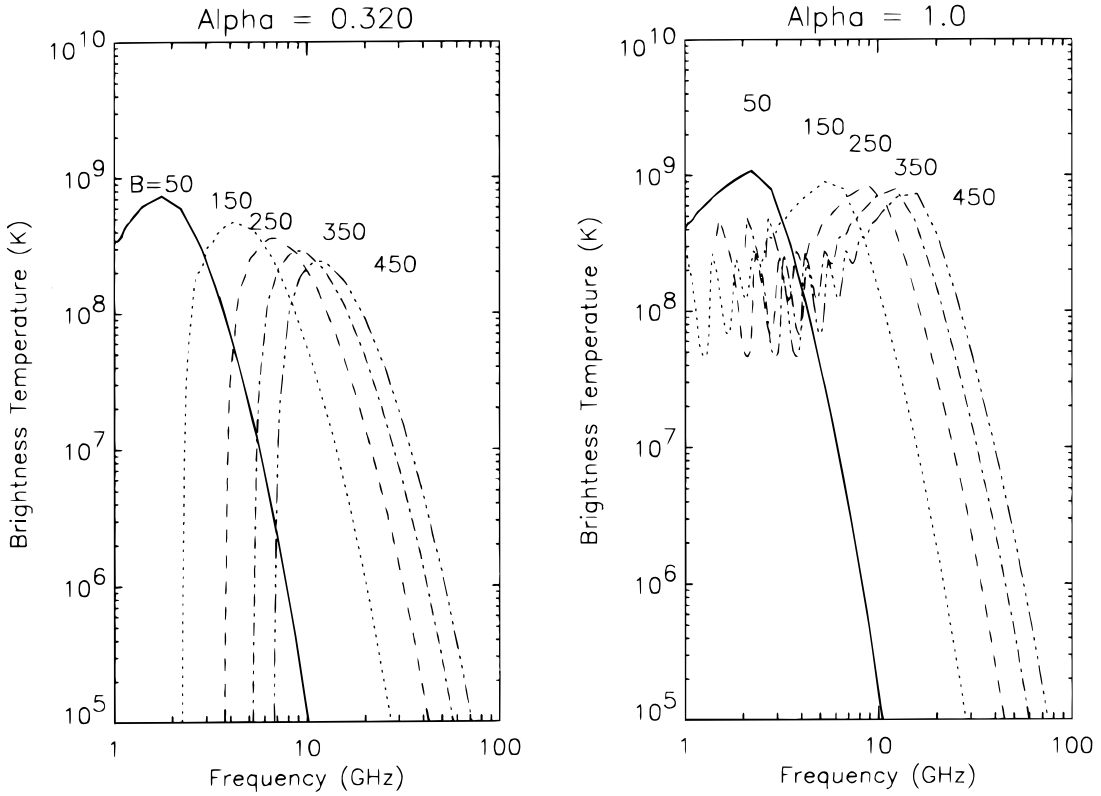

FIG. 5.—Effect on the brightness temperature spectrum of varying the magnetic field strength B from 50 to 450 G. The left panel shows the effect with Razin suppression, and the right panel without.

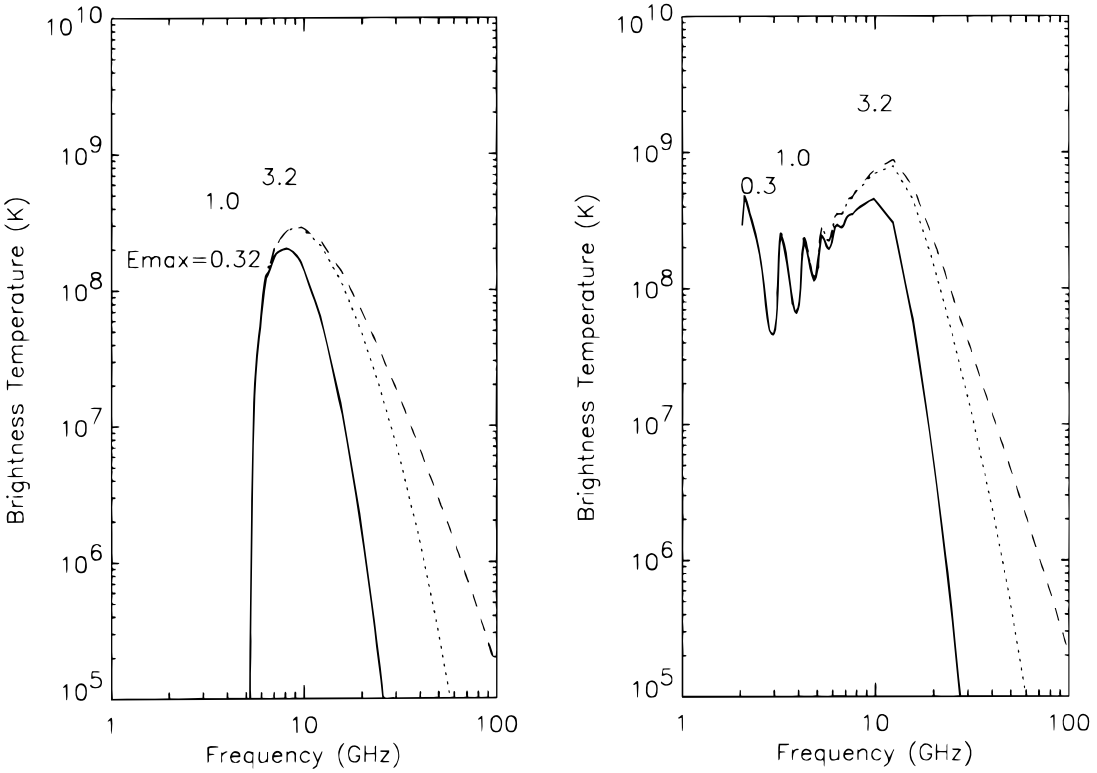

FIG. 6.—Effect on the brightness temperature spectrum of varying the high-energy cutoff in the electron energy distribution. The cutoff ranges from 0.32 MeV to 3.2 MeV. The left panel shows the effect with Razin suppression, and the right panel without.

the size of the source and the accelerated particle density. Although we expect the optical depth to the source to increase as the source grows during the flare, experience suggests that growth in the source size is accompanied by an increase in the source density, i.e., the expansion is homologous and the increased optical depth cannot be disentangled from the increase in particle density without an independent measurement of the source size along the line

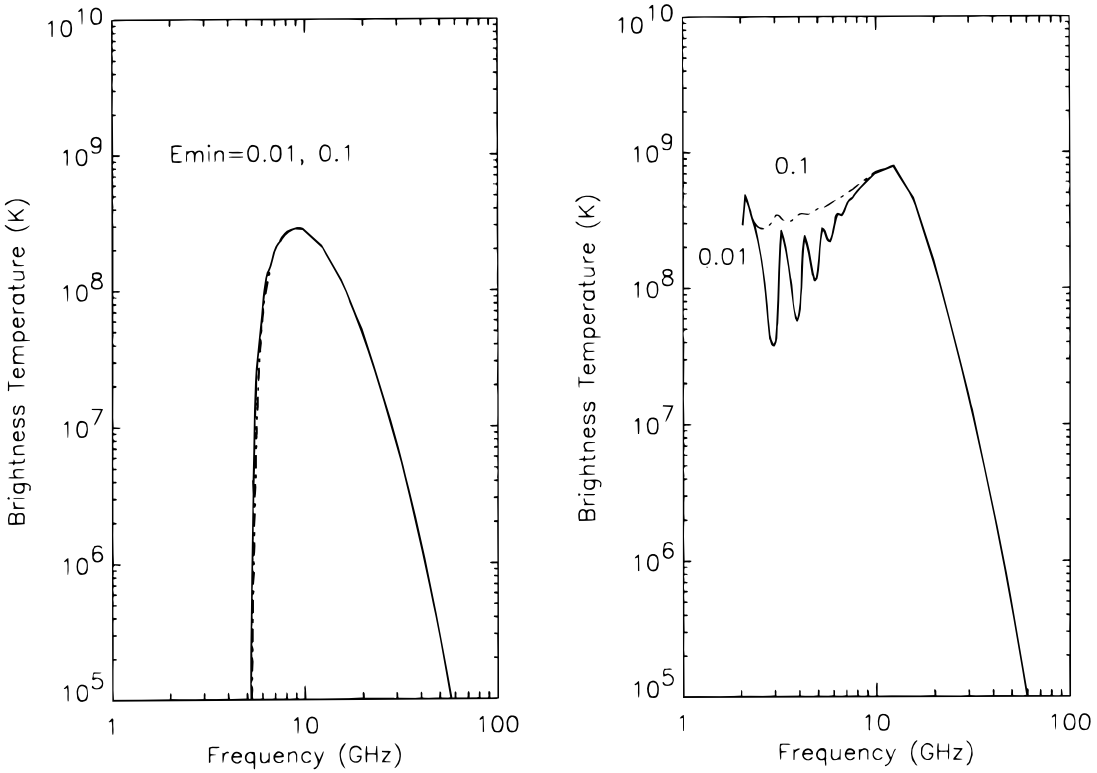

FIG. 7.—Effect on the brightness temperature spectrum of varying the low-energy cutoff in the electron energy distribution. The cutoff was varied from 0.01 MeV to 0.1 MeV with no appreciable effect on the spectrum. The left panel shows the effect with Razin suppression, and the right panel without.

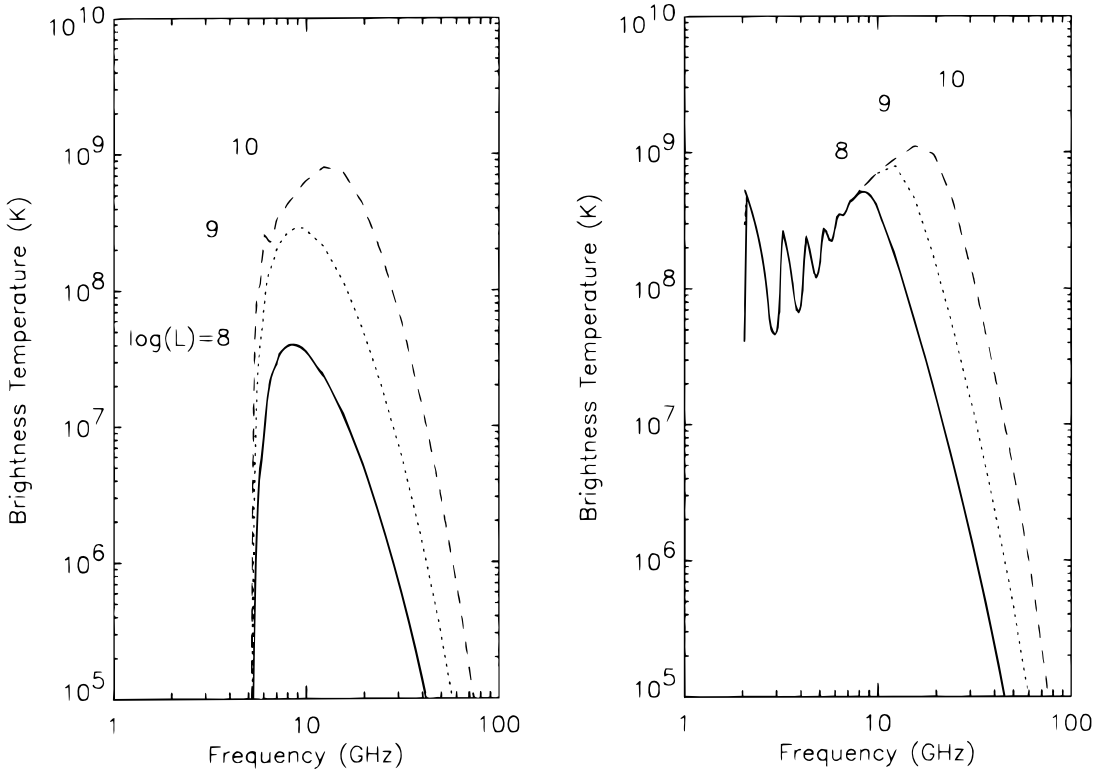

FIG. 8.—Effect on the brightness temperature spectrum of varying the path length to the source L. The effect is significant, but not distinguishable from varying the particle density or source size. The path length was kept fixed at 10^9 cm in the modeling. The left panel shows the effect with Razin suppression, and the right panel, without.

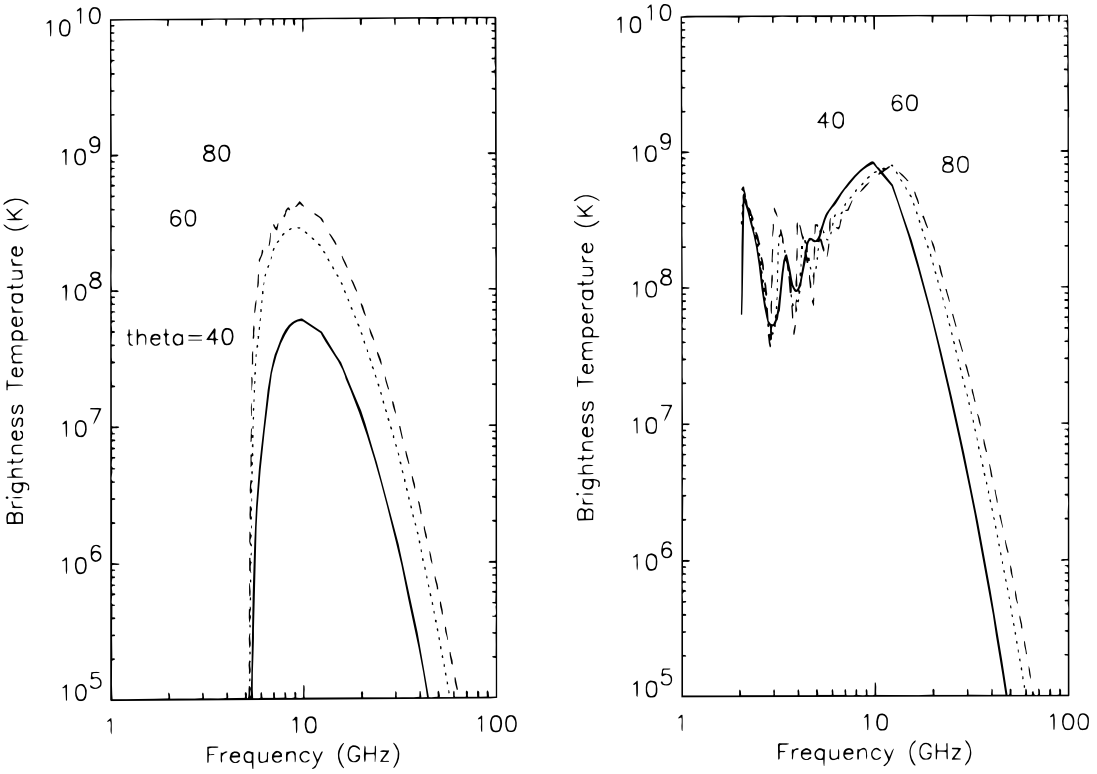

FIG. 9.—Effect on the brightness temperature spectrum of varying the viewing angle to the magnetic field θ. The effect is pronounced in the presence of Razin suppression. The viewing angle was not varied in the modeling since we consider it to be fixed, to first order, by the longitude of the source. The left panel shows the effect with Razin suppression, and the right panel, without.

of sight. We also note that for an increase in path length from 10^9 to 10^{10} cm^{-3} (and no variation in the accelerated particle density) the peak frequency shifts to higher frequencies, unlike the behavior we see for an increase in the accelerated particle density in the case with Razin suppression, so that a simple expansion of the source without an increase in the density of energetic particles could not account for the observed behavior of the brightness temperature spectrum. For simplicity in the modeling, then, we have attached all of the increase in source size to the increase in accelerated particle density. We must keep in mind, however, that the choice of a different path length to the source would alter the results of our modeling. A path length smaller than 10^9 cm, although unlikely based on typical observations, would mean that milder Razin suppression would be needed to fit the data.

Figure 9 shows the effect of varying θ, the angle between the line of sight and the magnetic field. The effect is substantial if the angle is less than 60°. However, we reiterate that we did not vary this angle in the modeling and consider the active region longitude as a good representation of this parameter.

In Figure 10 we summarize the effects in one figure, with arrows showing the direction of evolution of the spectrum corresponding to an increase in each of the eight parameters. The arrows indicate direction only, not relative magnitude of the effect. As mentioned earlier, we found that, in addition to the very pronounced effect of Razin suppression, the most important parameters are the accelerated particle density and (tied for third place in the hierarchy of influence) the exponent δ and the field B. The figure shows that α, θ, and N are the parameters capable of shifting the peak of the curve vertically, when Razin suppression is in effect. (Note that there are two arrows for N, as a reminder that the effect of N varies with the magnitude of this parameter.) In the case of $\alpha = 1$, with less or no Razin suppression, no single parameter shifts the curve purely in the vertical direction.

3.4. *Results of the Modeling*

Table 1 lists the best-fit parameters to the data, along with errors which are further discussed below. Figure 11 shows the results graphically. The data for the A, B, C, D, E, and F time samples are overlaid with plots of the best model fits to each curve. Figures 12, 13, and 14 show the evolution of the model parameters at the six times during the flare.

The errors quoted were determined by varying each parameter in turn, in a range centered on its best value for that fit. For example, starting with the C time sample best-fit parameters, we varied B and found that values from 320 to 390 G led to acceptable fits. This procedure was repeated for each free parameter. The errors show that the 16.4 GHz data points did not constrain the bandwidth of the curve very well. This is expected because of the higher noise and difficulty of imaging the source at this frequency.

In modeling the data we concentrated on fitting the curves for the A and C time samples, because they represented extremes in the physical conditions required to reproduce the observations. For example, the spectrum with peak brightness temperature near 10^9 K requires an accelerated particle density of at least 10^4 cm^{-3}; there does not seem to be any other way to achieve such high brightness temperature. This is in line with what other researchers have found; e.g., Kucera (1992) found $\sim 3 \times 10^3$ cm^{-3} and Willson et al. (1990) found $\sim 4 \times 10^6$ cm^{-3}. Increasing the accelerated particle density beyond a certain point,

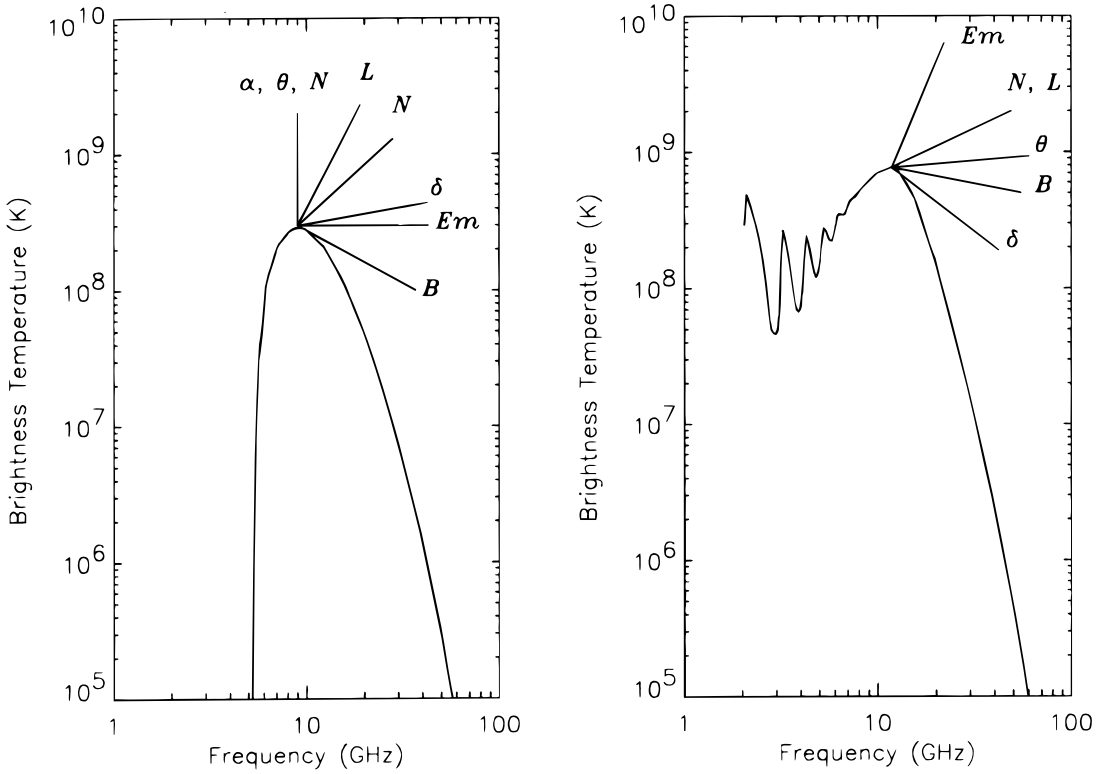

FIG. 10.—Effect of the physical parameters in the gyrosynchrotron model. Lines indicate the direction the curve evolves when the variable is increased. The lines indicate direction only, not relative magnitude of the effect. There are two lines for N in the left panel because increasing N can shift the curve both ways, depending on the value of N.

TABLE 1

BEST-FIT PARAMETERS

VARIABLE	TIME SAMPLE A	B	C	D	E	F
N	5.0×10^{28}	1.5×10^{29}	3.0×10^{30}	1.2×10^{30}	4.5×10^{29}	3.5×10^{28}
Error	$+1.2/-1.0 \times 10^{28}$	$+0.3/-0.2 \times 10^{29}$	$+0.3/-0.9 \times 10^{30}$	$+0.1/-0.2 \times 10^{30}$	$+0.2/-0.5 \times 10^{29}$	$+0.4/-0.5 \times 10^{28}$
n_e(accel).....	5.0×10^{2}	1.5×10^{3}	3.0×10^{4}	1.2×10^{4}	4.5×10^{3}	3.5×10^{2}
δ	4.0	4.0	4.0	4.0	4.0	4.0
Error	$+0.1/-0.1$	$+0.1/-0.1$	$+0.3/-0.5$	$+0.1/-0.2$	$+0.1/-0.1$	$+0.1/-0.1$
B	350	350	350	350	350	350
Error	$+10/-40$	$+40/-30$	$+40/-30$	$+20/-30$	$+40/-10$	$+40/-30$
E_{max}	0.398	0.631	1.000	0.501	1.000	1.000
Error	$+0.103/-0.082$	$+0.369/-0.130$	$+0.995/-0.369$	$+0.000/-0.103$	$+0.585/-0.206$	$+99/-0.206$
α	0.323	0.323	0.319	0.319	0.312	0.310
Error	$+0.003/-0.003$	$+0.006/-0.007$	$+0.008/-0.015$	$+0.004/-0.009$	$+0.004/-0.004$	$+0.005/-0.005$

however, does not increase the peak brightness temperature; a "saturation" effect is seen. Having fixed the accelerated particle density, a turnover frequency of about 10 GHz requires a magnetic field strength of about 350 G. The main problem with fitting time sample C is to get high enough brightness temperature and narrow enough bandwidth. If α is too high, resonant structures appear, in which case the bandwidth is very large. In the case of time sample A, the accelerated particle density must be reduced to fit the low brightness temperature spectrum, but the turnover frequency is then naturally low. The effect of Razin suppression is well demonstrated here, because while the higher T_b curves might be fitted with low Razin suppression if we allow a large bandwidth, for the lower T_b spectrum low Razin suppression leads to a low turnover frequency, which in turn would require a large boost in the magnetic field strength.

3.5. *Evolution of the Spectrum in the Absence of Razin Suppression*

In the absence of Razin suppression it is difficult both to fit the spectra and to find fits in which the dominant parameters (B, N, and δ) vary in a credible way from one time sample to the next. In Figure 15 we show an example of fits to the A and C spectra for the case in which the medium has no effect ($\alpha = 2$). For the C spectrum the parameters were $B = 400$ G, n_e(accel) $= 1.2 \times 10^3$ cm^{-3}, $\delta = 4$, and $E_{max} = 3.16$ MeV. For the A spectrum, which was much more difficult to fit, the parameters were $B = 700$ G, n_e(accel) $= 1.0 \times 10^{-4}$ cm^{-3}, $\delta = 7$, and $E_{max} = 1$ MeV. The C model has

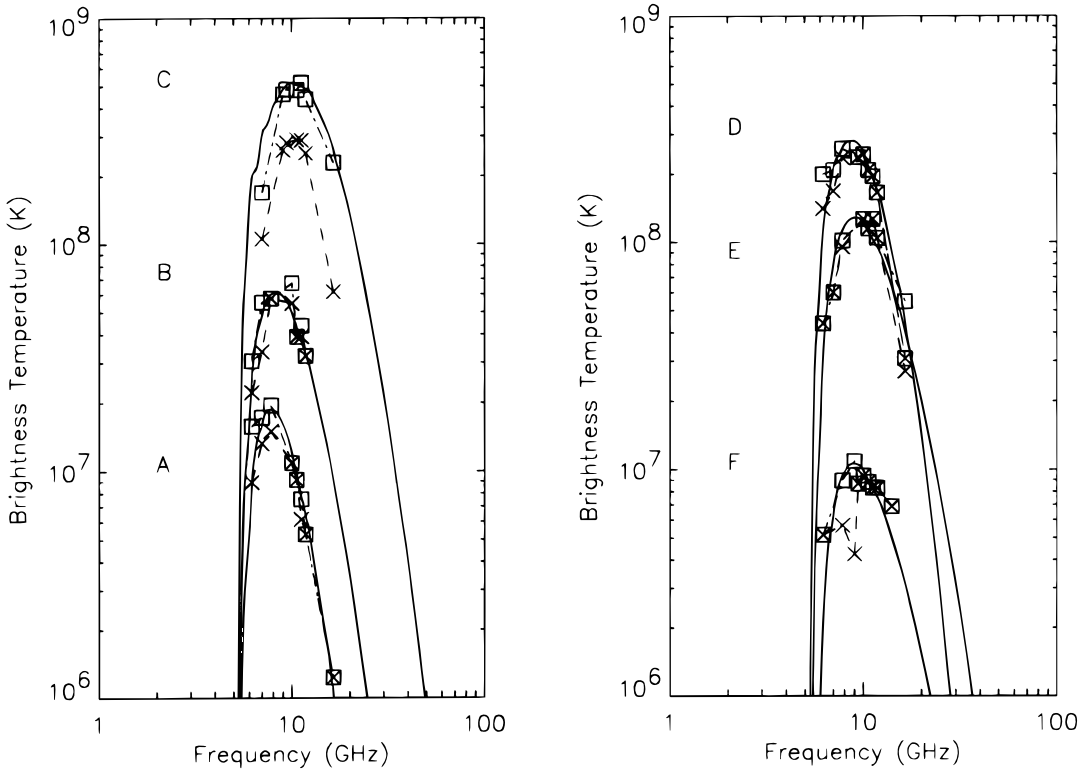

FIG. 11.—Overlay of the data for the A, B, C, D, E, and F times with the model fits

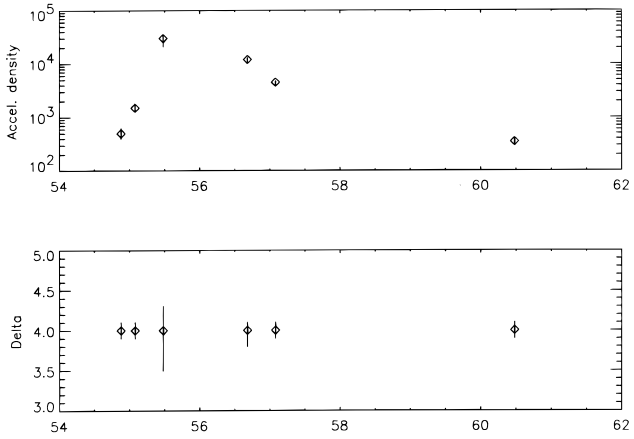

FIG. 12.—Evolution in time of the parameters of the model. Continued in Fig. 13.

too wide a bandwidth on the low-frequency side, but otherwise is not altogether unsatisfactory; on the other hand, the A model does not have the right shape at all. To get the total emission down to the right level the accelerated parti-

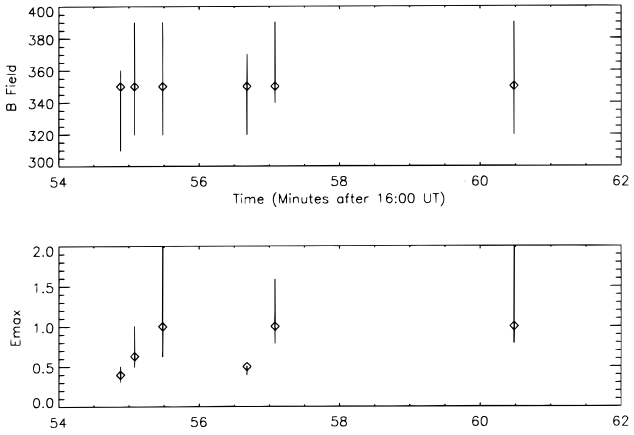

FIG. 13.—Evolution in time of the parameters of the model. Continued in Fig. 14.

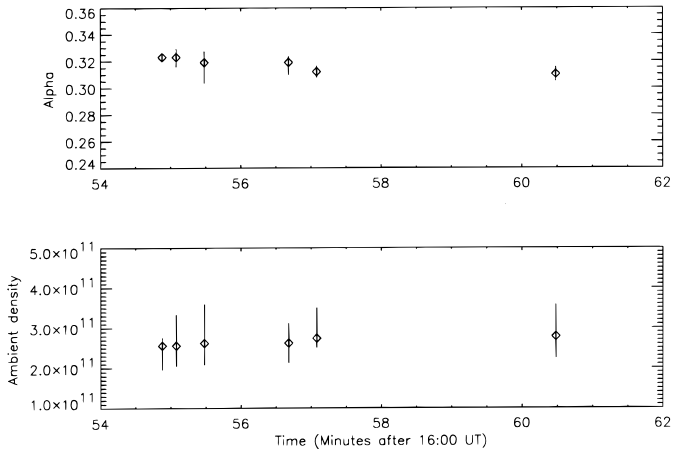

FIG. 14.—Evolution in time of the parameters of the model. Continued from Fig. 13.

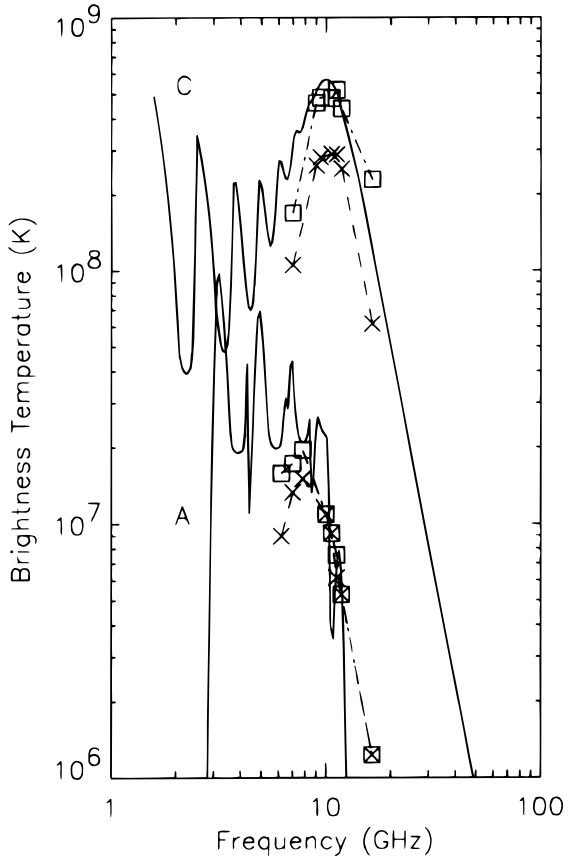

FIG. 15.—Examples of fits to the A and C spectra without Razin suppression.

cle density had to be reduced to extremely low levels (1.0×10^{-4} cm^{-3}); then the magnetic field and the exponent in the energy distribution function were manipulated to put the optically thin falloff at approximately the right frequency. The difficulty of fitting the spectra is strong evidence that a low-frequency cutoff is needed, and Razin suppression works very well to explain the shape and evolution of the spectra.

3.6. *Validity of the Simplifying Expressions of Dulk and Marsh*

We have shown that the effect of the medium alters the shape of the gyrosynchrotron spectra, not only on the low-frequency side but also in reducing the brightness temperature overall. In this section we check the applicability of the expressions of Dulk & Marsh when Razin suppression is at work. The equations to check are

$$T_{\rm eff} \sim 2.2 \times 10^9 10^{-0.31\delta} (\sin\theta)^{-0.36-0.06\delta} \left(\frac{\nu}{\nu_B}\right)^{0.5+0.085\delta}$$

and

$$\nu_{\rm peak} \sim 2.72 \times 10^3 10^{0.27\delta} \times (\sin\theta)^{0.41+0.03\delta} N L^{0.32-0.03\delta} B^{0.68\pm0.03\delta} .$$

For $\theta = 60°$, $\delta = 4$, $B = 325$ G, $n_e(\text{accel}) = 1.4 \times 10^3$ cm^{-3}, $L = 10^9$ cm, the expressions of Dulk & Marsh yield a peak frequency of 0.8 GHz, while, in fact, with Razin sup-

pression, the gyrosynchrotron model produces a peak frequency of about 7 GHz. Calculating the effective temperature at the peak frequency, the expressions of Dulk & Marsh give 7.7×10^8 K, while the same model gives a temperature of $\sim 2 \times 10^7$ K. The comparison shows that the effect of the medium is to produce an artificially high turnover frequency in the spectrum because the lower frequencies are suppressed.

4. DISCUSSION

We found that Razin suppression can solve the mystery of constant peak frequency in microwave flare spectra. The most important argument is that Razin suppression can explain not only an individual spectrum, but also the evolution in time of the spectra. Without Razin suppression we would have to vary several parameters (such as the magnetic field strength, the ambient density, and the index in the electron energy distribution function) in just the right way to keep the peak frequency constant (or nearly constant) while the brightness temperature varies over nearly 2 orders of magnitude. If Razin suppression is present, only the accelerated particle density is required to vary in order to change the peak brightness temperature. We do not rule out variations other than in the accelerated particle density, but we have shown that it is possible to model the evolution of the spectra with a simple variation in the accelerated particle density, once the remaining parameters (field strength, ambient density, electron energy distribution, and so forth) have been chosen appropriately.

The ambient density required in our model ($\sim 2 \times 10^{11}$ cm^{-3}) is higher than commonly assumed in models of the microwave emission. The ambient density is generally thought to lie in the range from 10^8 to about 3×10^{10} cm^{-3}, although recently some authors have reported higher densities. For example, Doschek (1994) used SXT and BCS data from *Yohkoh* to infer the temperature and density at the top of a flare loop and found $T \sim 10$–20×10^6 K and $n_e \sim 3.2 \times 10^{11}$ to 1.2×10^{12} cm^{-3}.

Benka & Holman (1992) also address the steep low-frequency slope and constant peak frequency in microwave burst spectra. They attribute the steep low-frequency slope to thermal absorption and interpret the constancy of the peak frequency in terms of a model of electron heating and acceleration in current sheets. In this model the evolution of the microwave spectra with constant peak frequency can be accounted for by a changing electric field strength, but this result is so far only qualitative.

One limitation of our modeling is that we did not investigate the emission with a nonisotropic pitch-angle (ϕ) distribution. Some investigations reported in the literature show that power is preferentially radiated in the direction $\phi = \theta$ (θ the angle between the magnetic field line and the line of sight) and that for large ($\phi - \theta$) the peak frequency and slopes of the spectra are affected (Tarnstrom 1976).

In future work it would be useful to have polarization data and to make use of this diagnostic in modeling with Razin suppression.

In summary, the flare scenario implied by our results is that the microwave emission takes place in a plasma of high ambient density. The accelerated particle density increases and decreases along with the peak brightness temperature during the flare, while δ and other parameters stay roughly constant. The *accelerated* particle density we infer is in line with that found by several other researchers as noted in § 3.4. We do not require the accelerated particle density to be a significant fraction, more than 1%, of the ambient density, as required in the models of Kaufmann et al. (1986) or McClements & Brown (1986). The high turnover frequency in the spectrum is determined by the suppression of low frequencies known as the Razin effect.

5. CONCLUSIONS

We have shown that the Razin effect can account for both the shape and evolution of a solar microwave burst spectrum observed at the Owens Valley Solar Array. Gyrosynchrotron emission up to approximately 10 GHz, far above the typical plasma frequency, is strongly suppressed, which leads to steep low-frequency slopes and artificially high, and constant, $\nu_{\rm peak}$. Razin suppression also accounts for the low brightness temperature of the burst during the early and late stages of the burst.

Our model is appealing because it provides a simple explanation for the shape and evolution of the spectrum. Without Razin suppression, several factors (e.g., the magnetic field in the burst region, or the electron energy distribution) must evolve in just the right way to keep the constancy of $\nu_{\rm peak}$ during the evolution of the burst. With Razin suppression, we have shown that only the density of accelerated electrons need vary. Further support for our model comes from the agreement between the ambient density and electron spectral index we infer from the microwave and X-ray data (Belkora 1995).

We sought to explain the burst spectrum and evolution by taking into account the Razin effect. We did not conduct a systematic review of all other possible sources of low-frequency cutoff. However, we found from analysis of the X-ray data for this flare that free-free absorption cannot account for the shape of the spectrum. Details of the multispectral analysis can be found in Belkora (1995) and in Belkora et al. (1996).

Klein (1987) and his colleagues investigated the Razin effect and the role of free-free and self-absorption in microwave sources. Many of our results support his conclusions. He finds, as we do, that the Razin effect creates a steep low-frequency slope in the burst spectrum when the ambient density is on the order of 10^{11} cm^{-3}. Our conclusions differ from his in that he requires source size $l \sim 10^7$ cm and a density of accelerated particles near 10^9 cm^{-3}, or about $10^{-2} \times n_e$(ambient). These differences may arise from Klein's interpretation of the millimeter flux data from which he inferred the column density of nonthermal electrons.

Our conclusions are important because they affect the interpretation of solar burst spectra. In particular, we must use care in using the spectral turnover frequency as an indication of the magnetic field strength in the burst region. Further analysis of the time evolution of brightness temperature spectra, such as can be obtained with the OVRO Solar Array, are needed. Silva et al. (1996) have invoked the Razin effect in their analysis of the 1994 August 18 flare from a compact loop.

This work was supported in part by NSF grant ATM 93-11416 and AST 93-14929 to California Institute of Technology. I thank Dale Gary, Dick McCray, Scott Robertson, and Fran Bagenal for their guidance and helpful suggestions.

REFERENCES

Belkora, L. 1995, Ph.D. thesis, Univ. Colorado
Belkora, L., Gary, D. E., & Kiplinger, A. 1996, in preparation
Benka, S. G., & Holman, G. D. 1992, ApJ, 391, 854
Cornwell, T., & Braun, R. 1989, in Synthesis Imaging in Radio Astronomy, ed. R. A. Perley, F. R. Schwab, & A. H. Bridle (San Francisco: ASP)
Doschek, G. A. 1994, in Proc. of Kofu Symposium, ed. S. Enome & T. Hirayama (Nagano, Japan: Nobeyama Radio Observatory
Dulk, G. A., & Marsh, K. A. 1982, ApJ, 259, 350
Ginzburg, V. L., & Syrovatskii, S. I. 1965, ARA&A, 3, 297
Hurford, G. H., Read, R. B., & Zirin, H. 1984, Sol. Phys., 94, 413
Kaufmann, P., Correia, E., Costa, J. E. R., & Zodi Vaz, A. M. 1986, A&A, 157, 11
Klein, K.-L. 1987, A&A, 183, 341
Kucera, T. 1992, Ph.D. thesis, Univ. Colorado
McClements, K. G., & Brown, J. C. 1986, A&A, 165, 235
Ramaty, R. 1968, J. Geophys. Res., 73, 3573
———. 1969, ApJ, 158, 753
Ramaty, R., & Lingenfelter, R. E. 1967, J. Geophys. Res., 72, 879
Ramaty, R., Schwartz, R. A., & Nakajima, H. 1994, ApJ, 436, 941
Silva, A. V. R., Gary, D. E., White, S. M., Lin, R. P., & de Pater, I. 1996, in preparation
Stähli, M., Gary, D. E., & Hurford, G. J. 1989, Sol. Phys., 120, 351
Tarnstrom, G. 1976, A&A, 49, 31
Willson, R. F., Klein, K.-L., Kerdraon, A., Lang, K. R., & Trottet, G. 1990, ApJ, 357, 662